Morphological Engineering of Inorganic Semiconductor VIS-Light-Driven Nanocatalysts: Experimental and Theoretical Understandings

Valentin Diez-Cabanes, Mariachiara Pastore

Morphological Engineering of Inorganic Semiconductor VIS-Light-Driven Nanocatalysts: Experimental and Theoretical Understandings

Valentin Diez-Cabanes,[1,*] *Mariachiara Pastore*[1,*]

[1] Université de Lorraine & CNRS, Laboratoire de Physique et Chimie Théoriques (LPCT), F-54000, Nancy, France

*Authors to whom correspondence should be addressed: valentin.diez-cabanes@univ-lorraine.fr; mariachiara.pastore@univ-lorraine.fr

KEYWORDS quantum confinement, facet engineering, tungsten oxide, metal halide perovskites, photocatalysis

ABSTRACT

Photocatalytic performances of inorganic semiconductors are mainly restrained by two factors: their low solar light harvesting capabilities and fast recombination of the generated charge carriers. Concerning the first point, some visible (VIS) light-driven catalysts, such as WO_3 and metal halide perovskites (MHPs), have emerged during the past years as promising alternatives to traditional TiO_2 based materials. Hole/electron pairs recombination, on the other hand, can be somehow controlled and slowed down via morphological engineering by rationally controlling the size and shape of the nanomaterial. In this work we discuss the recent breakthroughs achieved in the

photocatalytic applications of WO_3 and MHP nanostructures, highlighting the intertwined role played by facet engineering and quantum confinement effects. State-of-art theoretical methodologies and tools available to model these systems and their operating mechanisms are presented and their strengths and limitations discussed. With this information we point to the main challenges that theory and experiments should jointly address to develop more efficient solar light driven catalyst technologies.

1. Introduction

Nowadays, inorganic semiconductors are the most spread materials employed as photoactive components in photocatalytic devices.[1] In the last three decades, indeed, the enormous progresses in the synthesis and characterization of semiconductor nanostructures have incredibly boosted the performances of such energy systems. With respect to their bulk phases, nanoscale crystals show different opto-electronic and charge transport properties and, more importantly, these properties can be modulated by the proper choice of size and shape.[2] In this regard, one can engineer the nanostructure by preferentially exposing a given surface termination and employing a certain size and morphology with the idea of enhancing the interaction with the solvent, maximizing the charge generation and transport to finally promote the catalytic reactions. Surface termination effects have been found, indeed, to be crucial in dictating the photocatalytic behavior of the nanomaterials, such as their interfacial energetics and their stability.[3] Furthermore, by reducing the dimensions below the exciton Bohr radius of the material (which are often in the order of few nm for many semiconductors), the physical properties of the bulk phase do not longer hold because of quantum confinement effects and the nanostructure rather behaves as a molecule or a quantum dot (0D material) with a discrete number of energy states. Due to this, the absorption of the material

significantly increases, and less amount of matter is thus required to absorb the same amount of light.[4] Quantum effects may have a major impact on the photocatalytic performances, since in quantum confinement regime the electronic properties of the material are significantly modified.[5] For instance, quantum confinement effects offer the opportunity to target the desired properties i.e. a given redox potential, thus paving the way to catalyze certain reactions which are not energetically accessible by their bulk phase.[6] Another important consequence of dimensional reduction is the increase of the percentage of the atoms exposed to the reaction and the surface-to-volume ratio, thus yielding to an enhancement of the chemical activity and solubility when compared to their bulk counterparts.[7] In parallel, when decreasing the size of the nanostructure, the distance needed by the generated carrier to migrate towards the surface will be shortened as well, which considerably contribute to hamper the recombination of the charge carriers.[8] To summarize, morphological engineering can be beneficial in the field of photocatalysis for the following reasons: (*i*) the enlargement area-to-volume ratio, (*ii*) the enhancement of the active sites for reaction by facet selection, (*iii*) the shortening of the electron-hole diffusion paths, which considerably contributes to hamper the recombination of the charge carriers, (*iv*) the possible stabilization of the material in comparison with its corresponding bulk phase and (*v*) tuning the energy barriers with respect to the target redox potentials.

As a matter of fact, TiO_2 related nanostructures constitute by far the most studied photocatalytic materials,[9] although they present some inherent limitations, such as a wide bandgap and a relatively fast recombination of photogenerated charge carriers. Undoubtedly, the optical absorption in the UV region appears as the most critical feature, as TiO_2 is able to capture only a 3-5% of the energy of the solar spectrum. In view of this, many research efforts have been devoted to the design of new semiconductor materials which possess a better absorption in the VIS region.

In this context, other metal oxide semiconductors, exhibiting a relatively low bandgap (<3.2 eV), have represented a natural choice to replace TiO_2 as photoactive material in catalytic applications. Among all of them, WO_3 has been shown of particular interest since it possess photocatalytic properties which can be compared to those TiO_2.[10] Unfortunately, all metal oxide semiconductors still undergo relatively rapid charge carrier recombination, which partially limits the device's efficiencies, as discussed above. In this viewpoint, the growing research interest dedicated to metal halide perovskites (MHPs) has motivated their practical use in solar energy technologies. Due to their unique combination of properties such as suitable gaps (1.6-2.9 eV), high diffusion length, low exciton binding energy, easy processability and high defect tolerance,[11] these materials have emerged as a potential highly-efficient candidates for VIS-light-driven catalysis.[12,13]

Nonetheless, the design of new efficient functional materials requires a deep understanding of the main factors influencing the chemical-physical processes of interest, photocatalysis in our case, and the rationalization of the structure-properties relationships. In this context, theory can successfully assist experimental research on both the above-mentioned aspects by means of first-principle atomistic simulations based on the synergy of highly accurate methodologies and realistic structural models.

In this perspective paper, we have selected WO_3 and MHP nanomaterials as case studies to elucidate the current status of VIS-light-driven semiconductors and to draw their prospective future developments. First, based on the recent literature, we discuss the effects of both facet engineering and quantum confinement in the photocatalytic performance of WO_3 and MHP nanomaterials, featuring their advantages and limitations with respect to TiO_2. It is noteworthy to stress that, here, we only focus on the strategies employed to enhance the photocatalytic performance of the nanomaterial via morphological engineering; parallel approaches, such as

doping, defect control or hybrid heterojunctions (i.e., with nanocarbon or other inorganic materials, noble metal loading) will not be examined. Afterwards, we move our attention to the opportunities offered by computational modelling by discussing the main theoretical models and methods that has been developed to investigate the opto-electronic properties of photocatalytic nanomaterials, especially focusing on the still poorly studied WO_3 and MHP nanostructures. We conclude by pointing out the main queries that both theoretical and experimental communities must face together in the next future to develop efficient solar driven catalysis which can be exploited on a commercial large-scale.

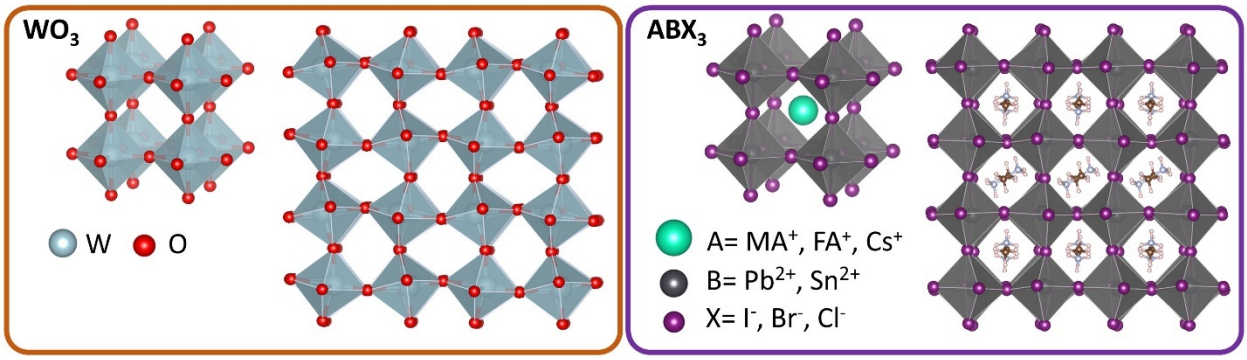

Figure 1. Perspective view of the cubic phase with the atom legends inset and lateral view of the pseudo cubic cells (triclinic for WO_3 and tetragonal for methylammonium lead iodide ($MAPbI_3$)) which are the most stable at room temperature, for WO_3 (orange) and prototype MHP (purple color) materials.

2. Results and discussion

WO_3 nanostructures

WO_3 presents a WO_6 corner and edge-shared octahedra, with the monoclinic I (m-WO_3) phase identified as the most stable one under usual conditions (see Figure 1 left). These materials exhibit

some important advantages with respect to TiO_2 such as high stability in extreme chemical environments (especially in the presence of strong oxidizing conditions) and absorption in the VIS region (absorption maximum at 480 nm).[14] The experimental band gap energy (E_g) of bulk WO_3 is about 2.6-2.8 eV, sensibly smaller than the corresponding value for bulk TiO_2 which lies in the 3.0-3.2 eV range.[15] This property allows WO_3 materials to absorb light at blue wavelengths, thus being able to capture ~12% of the solar energy spectrum, which is about four times larger with respect to TiO_2.[16] However, the conduction band (CB) edge of WO_3 lies very deep in energy (0.3-0.7 V vs RHE) compared to the reduction potential of O_2 (see Figure 2), favoring, in principle, the recombination of the photogenerated electron, drastically lowering the catalytic device performances. For the WO_3 monoclinic phase, the relative stability of the most commonly exposed surfaces terminations is (002) > (020) > (200), giving rise to cubic and rectangular sheet-like nanostructures, as represented in Figure 3-a and 3-b.[17,18] By making use of specific hydrothermal/solvothermal synthetic routes, one can tune the exposed facets of the nanomaterial, in order to enhance the reactivity of the targeted reaction by choice of the proper surface[19–21] and achieve different morphologies (see Figures 3-c and 3-d). Increasing the (002) surface area exposed to reaction has been, indeed, the most frequently employed strategy in the literature to enhance the photoactivity of WO_3 nanomaterials.[22] This methodology has also enabled the access to less stable facets, such as the (111) surfaces conforming octahedral like nanostructures (see Figure 3-c).[23] On the other hand, hexagonal WO_3 (h-WO_3) have recently emerged as new candidate materials for photocatalysis. As in the previous case, the (002), (020), (200) surfaces have been found to be the most active facets,[24] whereas different terminations can be obtained by following different synthetic methods. For instance, (001) exposed nanosheet[16,] and rectangular

prismoid (110) nanowires, with a remarkable photoactivity due to an enhanced hole mobility,[17] were recently reported (see Figures 3-e and 3-f).

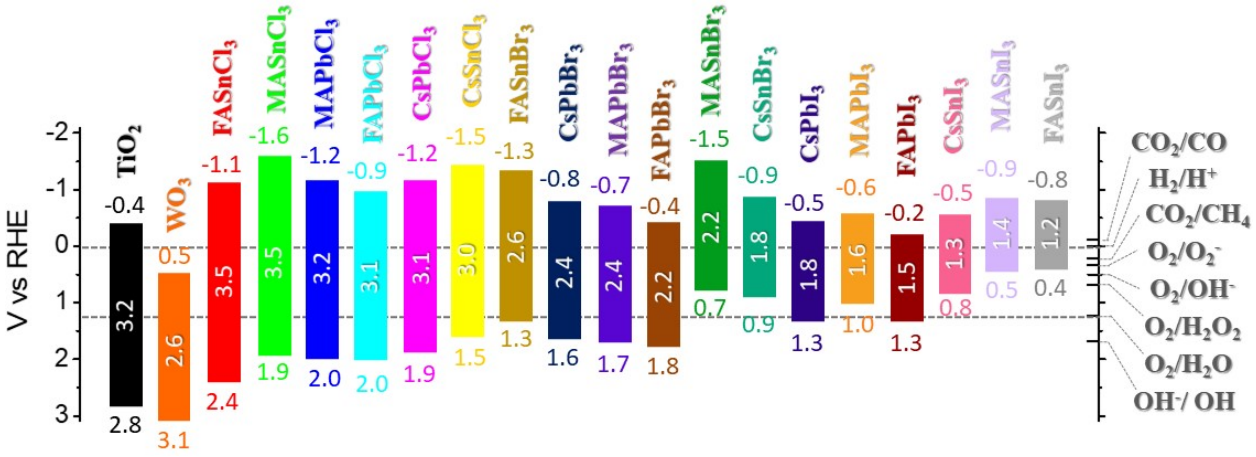

Figure 2. Band edge and gap energies for TiO_2, WO_3, and different MHPs families[27] taking as a reference the reversible hydrogen electrode (RHE) potential. The redox potentials for the most relevant photocatalytic reactions are indicated at the right part of the graph, whereas horizontal dashed lines were used to depict the H_2/H^+ and O_2/H_2O potentials.

Nevertheless, all the nanostructures mentioned above have dimensions of the order of several hundreds of nm, hence largely exceeding the exciton Bohr radius of WO_3 (~3 nm) and exhibiting a bulk like behavior. As a matter of fact, only few examples of WO_3 nanostructures owing such low dimensions have been reported in the literature. M.R. Waller *et al.* isolated two inorganic WO_3 octahedra layers by employing an exfoliation method, resulting in a quasi-2D material with a thickness of 0.75 nm.[28] In this case, quantum confinement yielded to a spurious effect in the photoelectrochemical water oxidation and electrical characteristics of the material (i.e. a small increase of 0.2 eV in the energy gap compared to the bulk phase was reported), thus resulting in similar performances with respect to the bulk.[28] As one may expect, quantum effects were found

much more prominent when involving the three dimensions of the material, in particular for quantum dot (QD) diameters below 1 nm, which lead to E_g values above 3.3 eV (see Figure 4-a),[29] hence making them less attractive from a photocatalytic point of view below that limit due to their absorption in the UV region. Notably, Tanaka et al synthetized a 1.4 nm diameter nanoparticle (NP) which displayed an enhanced benzene decomposition reactivity under UV exposure compared to the rates reached by the bulk material (see Figure 4-b).[30] This increase of the photocatalytic performance was attributed to the CB edge uplift above the single electron reduction potential of O_2, as it was later demonstrated by S. Cong and co-workers in similar WO_3 QDs (see Figure 4-c).[31]

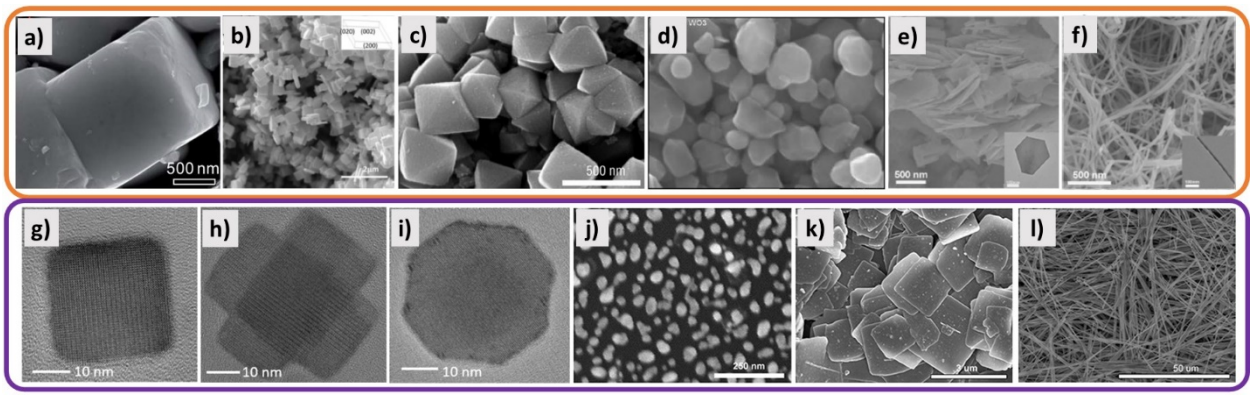

Figure 3. Summary of the morphologies for WO_3 and MHPs nanostructures. Scanning Electron Microscopy (SEM) images of a) quasi-cubic-like (200), (020) and (002)-exposed WO_3 NPs (Reprinted with permission from ref. 17 Copyright 2012 Royal Chemical Society)[17], b) rectangular (002)-exposed WO_3 nanoplate (Reprinted with permission from ref. 18 Copyright 2014 Royal Chemical Society)[18], c) (111)-delimited octahedra WO_3 NPs (Reprinted with permission from ref. 23 Copyright 2010 Royal Chemical Society)[23], d) colloidal spheric-like WO_3 NPs (Reprinted with permission from ref. 32 Copyright 2010 Elsevier)[32], e-f) hexagonal (001)-exposed WO_3 nanosheet and (110)-exposed WO_3 nanowires, respectively (Reprinted with permission from ref. 26

Copyright 2018 American Chemical Society)[26], g-i) (002), (110)-delimited cubic, (002), (110)-exposed hexapod and (002), (110), (112), (012), (100)- exposed polyhedral $CsPbBr_3$ NPs (Reprinted with permission from ref. 33 Copyright 2020 American Chemical Society)[33], j-l) colloidal, nanosheet and nanowire $MAPbI_3$ materials (Reprinted with permission from ref. 34 Copyright 2017 Elsevier)[34].

Despite that experimental evidence pointed to the potential of exploiting quantum effects in WO_3 in the field of photocatalysis, a clear picture of how these effects in different spatial directions affect the opto-electronic properties of the material, and the interfacial properties in the currently synthetized nanostructures, is still missing. To fill this gap, we set up a reliable computational approach to predict the structural and opto-electronic properties of realistic WO_3 NPs with different sizes and morphologies, establishing some important design rules for boosting their photocatalytic properties.[35] Our results revealed that cubic $(WO_3)_n$ nanostructures owing a number of units in the range $100 > n > 150$ (1.4-1.8 nm of lateral size) are optimal for photocatalytic purposes in view of their larger stability and favorable energetics with respect to the O_2 evolution potential, while maintaining their absorption in the VIS region.[35] Despite the electronic properties of the WO_3 nanostructures can be finely tuned via controlling their morphology, these materials still suffer from some fundamental drawbacks. Firstly, the carrier transport in WO_3 materials (and in all metal oxides) is hindered by the high hole localization on the O(2p) states; this facilitates the charge recombination, reducing the device's performance. Moreover, despite WO_3 possess a smaller energy gap with respect to TiO_2, this value is still far to be optimal for absorbing light in the solar spectrum. In such scenario, both constraints can be overwhelmed by employing MHP semiconductors, whose main advantages and limitations as potential photocatalyst will be discussed in detail in the next section.

MHP nanostructures

Perovskites present an ABX_3 chemical structure, displaying similar BX_6 octahedral geometries as WO_3, but with A cations occupying the center of the octahedra cavities (see Figure 1 right). The chemical constituents of MHPs are typically methylammonium (MA^+), formamidinium (FA^+), or Cs^+ as A cations, Pb^{2+} or Sn^{2+} atoms as B metal cations, and a halide (I^-, Br^- and Cl^-) as X anion. As we have pointed above, their excellent transport properties, together with the possibility to precisely tune the position of the valence/conduction band (VB/CB) edges via chemical engineering of its components (see Figure 2), make MHPs appearing as suitable candidates to replace TiO_2 catalysts. Although its ionic lattice is at the origin of the most relevant properties of MHPs, it is highly unstable in many chemical environments, especially in polar solvents, thus hindering their practical use in catalysis. Therefore, only few chemical reactions catalyzed by MHPs have been reported, including H_2 generation from saturated halo acid solutions, CO_2 reduction and organic synthesis in low-polarity solvents.[13] In this context, dimensional confinement of perovskites structures has been a very active filed of research during the past years in view of the significant stabilization of the material with respect to the bulk phase.[36] For perovskite nanostructures, quantum confinement effects enhance electron-hole interactions and stabilize excitonic emission within a broad range of temperatures. As a result, many recent studies have been dedicated to the use of these material in emitting devices,[37] whereas much lower attention has been paid to their photocatalytic applications.[12,13] To date, full inorganic $CsPbX_3$ (X = I, Br, Cl) related nanostructures represent the most studied family of metal halide perovskites,[38] and they are often employed to catalyze CO_2 reduction reactions.[39] The most common exposed facets for these structures are (110) and (002) surfaces, corresponding to their perovskite orthorhombic phase. However, these exposed surfaces are not necessarily the most reactive facets.

For instance, S. Shyamar *et al.* synthetized a non-cubic multifaceted nanostructure which, despite showing lower photoluminescence quantum yields (PLQY), lead to larger photocatalytic performances with respect to its cubic counterpart (see Figures 3 g-i).[33] Since the exposed facets are usually perpendicular to each other, perovskite nanostructures often exhibit a prismoid-like shape with different dimension lengths (cuboid, nanosheet, nanorods). For this families of nanostructures, their electronic structure were finely determined by its smallest dimension, rather than their specific shape.[40] Nevertheless, both size and shape of the nanostructures can be finely tuned via hot injection and ligand assisted re-precipitation synthesis (see Figure 3 j-l),[41] offering different possibilities to properly tune their size to optimize the photocatalytic performances. J. Hou *et al.* found, for instance, that cubic-shaped $CsPbBr_3$ displayed the largest CO_2 reduction rates for a lateral dimension equal to 8.5 nm (see Figure 4-d).[42] Interestingly, quantum confinement effects do not so largely affect the E_g values, as compared with the WO_3 NPs. For instance, a bandgap increase of 0.34 eV was observed when moving from 1 nm-diameter to the bulk-like $MAPbI_3$ nanocrystals (see Figure 4-e),[43] whereas for the same range of sizes, WO_3 QDs exhibited a gap increase of 0.7 eV.[29] In this viewpoint, J. Butkus *et al*. indicated that despite the charge dynamic of $CsPbBr_3$ QDs is changing below a size of 7 nm with respect to the bulk behavior, only for lateral lengths lower than 4 nm strong quantum effects are present, being the carrier dynamics driven by discrete density of states (see Figure 4-f).[44]

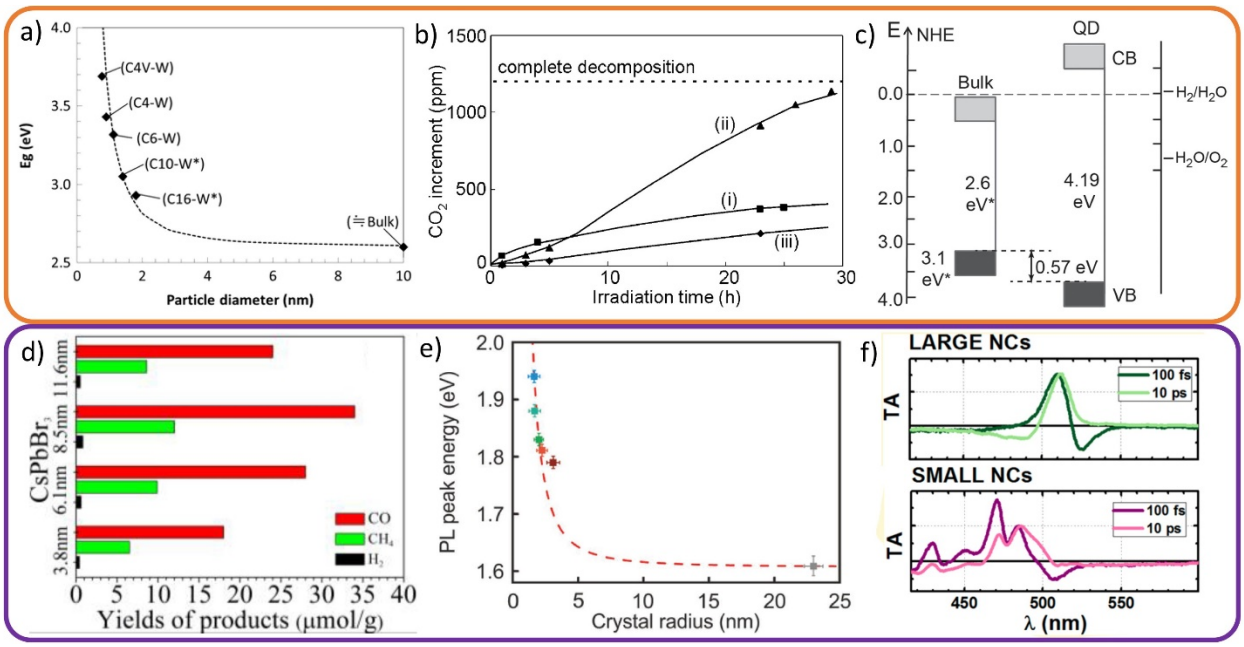

Figure 4. Quantum confinement effects in WO_3 and MHPs nanostructures: a) Evolution of E_g with the WO_3 QD size as calculated by Tauc plot, where the solid lines represent the theoretical values obtained Brus equation (Reprinted with permission from ref. 29 Copyright 2013 Royal Chemical Society)[29]; b) CO_2 formation rates from benzene photodegradation for (i) bulk WO_3, (ii) a 1.4-nm-diameter and (iii) 1.8-nm-size QD WO_3 (Reprinted with permission from ref. 30 Copyright 2010 Royal Chemical Society)[30]; c) band edges energies with respect to Normal Hydrogen Electrode (NHE) potential for the bulk WO_3 and a 1.6 nm diameter WO_3 QD, as estimated by X-ray photoelectron spectroscopy (XPS) and Tauc plot measurements (Reprinted with permission from ref. 31 Copyright 2014 Wiley-VHC)[31]; d) light-driven CO_2 reduction rates into CO, CH_4 and H_2 products achieved by using 3.8, 6.1, 8.5 and 11.6 nm-size $CsPbBr_3$ QDs as catalysts (Reprinted with permission from ref. 42 Copyright 2017 Wiley-VHC)[42]; e) PL energies as a function of the $MAPbI_3$ NPs size (Reprinted with permission from ref. 43 Copyright 2017 Wiley-VHC)[43]; f) Normalized transient absorption (TA) spectra with 10 ps and 100 ps for 8.6-nm (green) and 4.1-

nm-size (purple) $CsPbBr_3$ NPs (Reprinted with permission from ref. 44 Copyright 2017 American Chemical Society)[44].

3. Modelling inorganic semiconductor nanostructures

Structural Models

As a matter of fact, most of theoretical models dealing with the surface termination effects consists of slab models which are constructed by cutting the bulk phase along a desired direction and then selecting one given termination (see Figure 5 a-b). In the practice, these models are often exploited to analyze the relative stabilities and electronic properties for the different surfaces exposed for a given material.[45,46] Moreover, this approach can be also employed to investigate the heterointerfaces of the photoactive semiconductor with another materials or with the solvent implicated in the photocatalytic reaction.[47] The description of the solvent can rely on a full implicit description of the medium, static calculations of few explicit solvent molecules (usually the first adsorbed layer), hybrid implicit/explicit models till to a full dynamic treatment of various solvation shells by means of Molecular Dynamics (MD) techniques.[48] Despite these approaches are well established and implemented in TiO_2/solvent interfaces,[49,50] much lower interest has been devoted to WO_3 and MHPs interactions with solvents. For WO_3 these approaches have been used to examine the adsorption energies of solvent molecules on different surfaces,[51–53] whereas for MHPs most of the studies deal with the degradation of the perovskite structure in water environment.[54–56] Notably, these models permit also to tackle the different reaction paths followed by the solvent molecules adsorbed on the semiconductor surface. As an example, L. Wang *et al*. found that H_2 evolution reaction on $MAPbI_3$ surfaces from halide acid solution consisted of two-step Pb-

activated mechanism assisted by the organic cation, which forms an intermediate lead hydride state.[57]

On the other hand, slab models allow to treat quantum confinement only along one dimension, and if one wants to properly study quantum confinement effects in the three spatial directions, realistic 0D material models have to be built. These systems are often constructed by following top-down or bottom-up approaches,[58] and their size can span from few chemical units to nanomaterials of few nm size that mimics the bulk properties. This procedure, recently implemented by us for WO_3 (see Figure 5-c),[35] although much more cumbersome than the 2D slab approach in the judicious design of the structural models, enables to get a complete picture of the interplay of size and shape of the nanostructures in the opto-electronic properties of the material. In the case of MHPs, both small[59,60] and large[61,62] cluster models (see Figures 5 d-e) have been employed to explore the opto-electronic properties of perovskite materials, but the systematic investigation of the size-shape relationship has never been tackled.

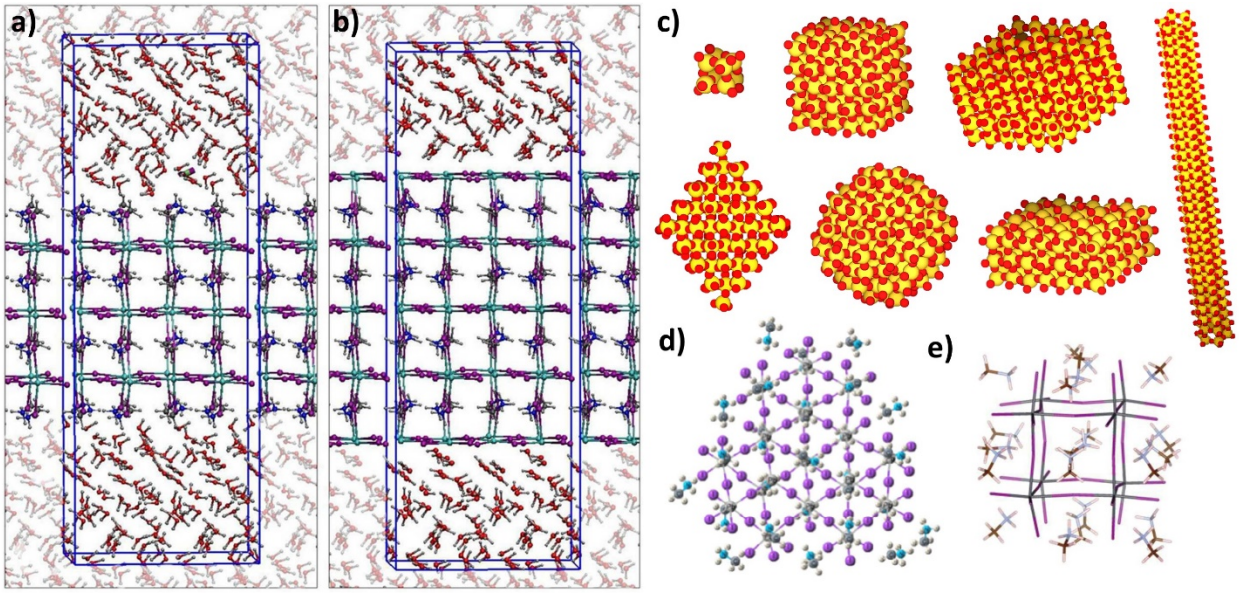

Figure 5. Slab and cluster theoretical models for WO_3 and MHPs materials. Perspective views of the a) MAI- and b) PbI_2-terminated $MAPbI_3$ slab solvated in water (Reprinted with permission from ref. 54 Copyright 2015 American Chemical Society)[54]; c) cubic $(WO_3)_8$ and $(WO_3)_{125}$, hexagonal nanosheet $(WO_3)_{147}$ and nanowire $(WO_3)_{186}$, octahedral $(WO_3)_{129}$, spherical $(WO_3)_{147}$ and rectangular $(WO_3)_{147}$ NPs (from the top left to the bottom right); and d) $MA_{25}Pb_{19}I_{63}$ (Reprinted with permission from ref. 61 Copyright 2017 American Chemical Society)[61] and e) $MA_{20}Pb_8I_{36}$ (Reprinted with permission from ref. 60 Copyright 2016 Royal Chemical Society)[60] perovskite cluster models.

Concerning the description of NP/solvent interactions, computationally less demanding implicit models are usually preferred when targeting optical and electronic properties,[63] despite the fact that one needs to consider at least few explicit solvent molecules up to few solvent layers, together with thermal effects, to characterize the catalytic mechanism. In the latter case, the size of the simulation (easily few thousand of atoms) becomes unaffordable for full first principle methodologies, and parametrized cheaper approaches, possibly combined with machine learning schemes, are the methods of choice.[64]

Ground and Excited State Properties

In view of the medium-to-large size of the described systems, Density Functional Theory (DFT) methods are the most common tool to access to their electronic structure due to the favorable ratio between accuracy and moderate computational cost. Unfortunately, standard DFT methods (i.e. Generalized Gradient Approximation (GGA) functionals) usually fail in properly describing the electronic structure of inorganic semiconductors (especially their energy gap)[65] hence making necessary to go beyond the mean-field description including both relativistic and many body

interaction effects (i.e. via hybrid functionals or *GW* approximation).[66] The study of the excited state properties of these systems becomes a crucial issue in view of the strong e-h interactions prompted by the quantum confinement effects. The most commonly used approach to this end is the Time-Dependent DFT (TD-DFT) method. Despite its overall good performances, the results given by TD-DFT are highly dependent on the choice of the functional and the type of system under study.[67] In this regard, during the last years the combination of *GW* approximation and Bethe Salpeter Equation (*GW*/BSE) has emerged as a highly accurate but still affordable method to treat ground and excited properties, respectively, in small and medium size systems (up to 200 atoms).[68] Indeed, the fast development of this methodology in both Solid State and Quantum Chemistry communities has allowed its use in the investigation of quantum confinement effects in perovskites. In this regard, G. Giorgi et al demonstrated that many-body Coulomb interactions are at the origin of the excitonic nature of layered perovskites.[69] On the other hand, all methods mentioned till now are used to tackle small and medium size structures, hence becoming computationally prohibitive for large systems owing several thousand of atoms. In this context, lower computationally costly methodologies have been developed with the aim of investigating both ground and excited state properties at the nanoscale. Among them, tight binding methods based on semi-empirical and theoretical data are the most commonly employed approaches. In our cases of interest, despite tight binding models have been established in the study of perovskite materials,[70] their practical use in the study of the electronic structure of finite nanostructures is not so extended as it is the case of other metal oxide nanoparticles.[71,72] Interestingly, tight binding models can be combined to other approaches aimed at simulating excite state dynamics (i.e. surface hopping) in order to evaluate the excitonic behavior of nanomaterials.[73] One complementary strategy to reduce the computational burden of the calculation relies on describing with classical

potential functions those regions of the system which are of lower interest (the so-called QM/MM approach).[74] This technique is especially useful when dealing with solvent/semiconductor interfaces, as mentioned above, where those solvent layers lying far from the surface are treated at the classical level; and it has enabled to study the interaction of large semiconductor nanostructures with its solvent environment.[75]

As a matter of fact, both the realistic description of the explicit solvent and the time evolution of the charge carriers are usually treated by means of MD schemes. In this context, accurate *ab-initio* MD (AIMD) represents the most largely employed approach to investigate charge dynamics in semiconductor/solvent interfaces and semiconductor quantum dots. For instance, based on AIMD simulations, J. Vogel *et al.* pointed to multiple-electron generation (MEG) as the main excited state relaxation mechanism followed by $MAPbI_3$ QDs,[61] whereas J. He *et al*. demonstrated that doping $CsPbBr_3$ QDs with iodine atoms extended the charge carrier lifetime by a factor of 5 due to the reduction of the electron-phonon coupling.[76] Nevertheless, due to their high computational cost, these simulations can be applied only to cells with lateral dimensions in the order of few Å and in timescales ranging from few tens to few hundreds ps. In this respect, Force Field (FF) MD emerges as an alternative to investigate larger systems (few hundreds of nm) and to track physical processes occurring in larger timescales (up to few μs). Despite this type of dynamics has been successfully applied to capture the change of the phase transitions with the temperature in bulk MHPs,[77] it has never been implemented for slabs or nanostructured materials. Very interestingly, prior to a QM parameterization, FF simulations can be also applied to analyze the reactions taking place at the semiconductor/solvent interface. Also known as reactive FF (reaxFF) technique, this procedure has been used in the past to track the decomposition of water on TiO_2 surfaces.[78] Before closing this section, it is noteworthy to mention that rapid development

of machine learning algorithms has opened the path to their implementation in the field of photocatalysis, for example, by predicting the catalytic activity of realistic semiconductor nanoparticles.[79]

4. Conclusions and prospective

Despite showing in principle a better photoactivity under solar irradiation, the photocatalytic performances achieved by WO_3 and MHPs are still far from the record efficiencies registered with TiO_2 based catalysts. For instance, some of the largest photocatalytic rates reported for H_2 generation with TiO_2, WO_3 and MHPs are equal to 1.97,[80] $2.9*10^{-3}$,[81] and $3.7*10^{-3}$ mol g^{-1} h^{-1},[82] respectively. Despite such a scenario, morphological engineering still provides a huge margin to improve the photocatalytic activity of WO_3 and MHPs nanomaterials. Recent advances in synthetic methods have open the possibility to have a finely control over the shape and size of the nanostructure, but the rational understanding of the interconnected role played by these two factors in the photogenerated charge carriers, and their implication in the photocatalytic design, is still far from being understood. From an experimental point of view, most of the studies have focused on the size evolution of the energy gap of the QDs, whereas much effort should be ideally put to address the rationalization of charge dynamics in the quantum confinement regime and the influence of the morphology and the interaction with the solvent. As an example, in perovskite QDs both PL and photocatalytic performance seemed to decrease in the quantum confinement regime, what traditionally has been attributed to the loss of the defect tolerance showed by perovskite QDs[83] due to the energy gap increase induced by quantum confinement. Despite these states are thought to form shallow traps, their influence in the dynamics and non-radiative recombination should be investigated in detail. Theory has been probed a powerful tool to elucidate this one and many another pending issues in the field. The conjunction of highly accurate and

unbiased methodologies such as the *GW*/BSE method and realistic treatment of the solvent/semiconductor interactions via large-scale MD simulations are at the heart of the rational understanding of charge carrier generation and recombination processes. Furthermore, the development of accurate FF parameters and tight binding methods for the slab and cluster models can open the possibility to treat realistic-size structures with an affordable computational cost and to simulate longer timescale phenomena such as slow carrier recombination. In this context, machine learning methodologies have shown their great potentialities for providing an unbiased and easy parametrization with at a reduced computational cost. Still, the construction of realistic models to simulate photocatalytic cells is in need of some experimental feedback, especially for determining the nature of the solvent/semiconductor interactions. Finally, upon reaching a precise morphological control and a deep knowledge of the physical process driving the charge generation of these nanomaterials, one possible route to improve their photocatalytic efficiency may consist in building optimized heterojunctions by combining nanostructures with optimal sizes and morphologies to minimize the recombination of the generated carriers. In summary, a synergic theorical and experimental research effort to provide a practical understanding of the subjects presented above will definitely constitute a breakthrough in the design of VIS-light-driven catalysts, and more general, in the development of green energy technologies.

AUTHOR INFORMATION

Corresponding Authors

Valentin Diez-Cabanes- *Université de Lorraine & CNRS, Laboratoire de Physique et Chimie Théoriques (LPCT), F-5400, Nancy, France*. ORCID: https://orcid.org/0000-0002-6234-2749. Email: valentin.diez-cabanes@univ-lorraine.fr

Mariachiara Pastore- *Université de Lorraine & CNRS, Laboratoire de Physique et Chimie Théoriques (LPCT), F-5400, Nancy, France.* ORCID: https://orcid.org/0000-0003-4793-1964. Email: mariachiara.pastore@univ-lorraine.fr

Notes

The authors declare no competing financial interest.

ACKNOWLEDGMENT

V.D.-C. is grateful to the financial support given by the COMETE project (COnception in silico de Matériaux pour l'EnvironnemenT et l'Energie), which is co-funded by the European Union under the program 'FEDER-FSE Lorraine et Massif des Vosges 2014-2020. M.P. acknowledges ANR JCJC HELIOSH2 (ANR-17-CE05-0007-01) project for the financial support.

REFERENCES

(1) Xu, C.; Ravi Anusuyadevi, P.; Aymonier, C.; Luque, R.; Marre, S. Nanostructured Materials for Photocatalysis. *Chem. Soc. Rev.* **2019**, *48*, 3868–3902.

(2) Chen, X.; Li, C.; Grätzel, M.; Kostecki, R.; Mao, S. S. Nanomaterials for Renewable Energy Production and Storage. *Chem. Soc. Rev.* **2012**, *41*, 7909–7937.

(3) Wang, S.; Liu, G.; Wang, L. Crystal Facet Engineering of Photoelectrodes for Photoelectrochemical Water Splitting. *Chem. Rev.* **2019**, *119*, 5192–5247.

(4) Alivisatos, A. P. Semiconductor Clusters, Nanocrystals, and Quantum Dot. *Science* **1996**, *271*, 933–936.

(5) Edvinsson, T. Optical Quantum Confinement and Photocatalytic Properties in Two-, One- and Zerodimensional Nanostructures. *R. Soc. Open Sci.* **2018**, *5*,180387.

(6) Li, A.; Wang, T.; Li, C.; Huang, Z.; Luo, Z.; Gong, J. Adjusting the Reduction Potential of

Electrons by Quantum Confinement for Selective Photoreduction of CO2 to Methanol. *Angew. Chemie* **2019**, *131*, 3844–3848.

(7) Burda, C.; Chen, X.; Narayanan, R.; El-Sayed, M. A. Chemistry and Properties of Nanocrystals of Different Shapes. *Chem. Rev.* **2005**, *105*, 1025–1102.

(8) Alivisatos, A. P. Perspectives on the Physical Chemistry of Semiconductor Nanocrystals. *J. Phys. Chem.* **1996**, *3654*, 13226–13239.

(9) Nakata, K.; Fujishima, A. TiO2 Photocatalysis: Design and Applications. *J. Photochem. Photobiol. C Photochem. Rev.* **2012**, *13*, 169–189.

(10) Quan, H.; Gao, Y.; Wang, W. Tungsten Oxide-Based Visible Light-Driven Photocatalysts: Crystal and Electronic Structures and Strategies for Photocatalytic Efficiency Enhancement. *Inorg. Chem. Front.* **2020**, *7*, 817–838.

(11) Manser, J. S.; Christians, J. A.; Kamat, P. V. Intriguing Optoelectronic Properties of Metal Halide Perovskites. *Chem. Rev.* **2016**, *116*, 12956–13008.

(12) Huang, H.; Pradhan, B.; Hofkens, J.; Roeffaers, M. B. J.; Steele, J. A. Solar-Driven Metal Halide Perovskite Photocatalysis: Design, Stability, and Performance. *ACS Energy Lett.* **2020**, *5*, 1107–1123.

(13) Han, C.; Zhu, X.; Martin, J. S.; Lin, Y.; Spears, S.; Yan, Y. Recent Progress in Engineering Metal Halide Perovskites for Efficient Visible-Light-Driven Photocatalysis. *ChemSusChem* **2020**, *13*, 4005–4025.

(14) Zheng, H.; Ou, J. Z.; Strano, M. S.; Kaner, R. B.; Mitchell, A.; Kalantar-Zadeh, K. Nanostructured Tungsten Oxide - Properties, Synthesis, and Applications. *Adv. Funct. Mater.* **2011**, *21*, 2175–2196.

(15) Grätzel, M. Photoelectrochemical Cells. *Nature* **2001**, *414*, 338–344.

(16) Huang, Z. F.; Song, J.; Pan, L.; Zhang, X.; Wang, L.; Zou, J. J. Tungsten Oxides for Photocatalysis, Electrochemistry, and Phototherapy. *Adv. Mater.* **2015**, *27*, 5309–5327.

(17) Xie, Y. P.; Liu, G.; Yin, L.; Cheng, H. M. Crystal Facet-Dependent Photocatalytic Oxidation and Reduction Reactivity of Monoclinic WO3 for Solar Energy Conversion. *J. Mater. Chem.* **2012**, *22*, 6746–6751.

(18) D'Arienzo, M.; Armelao, L.; Mari, C. M.; Polizzi, S.; Ruffo, R.; Scotti, R.; Morazzoni, F. Surface Interaction of WO3 Nanocrystals with NH3. Role of the Exposed Crystal Surfaces and Porous Structure in Enhancing the Electrical Response. *RSC Adv.* **2014**, *4*, 11012–11022.

(19) Wang, S.; Chen, H.; Gao, G.; Butburee, T.; Lyu, M.; Thaweesak, S.; Yun, J. H.; Du, A.; Liu, G.; Wang, L. Synergistic Crystal Facet Engineering and Structural Control of WO3 Films Exhibiting Unprecedented Photoelectrochemical Performance. *Nano Energy* **2016**, *24*, 94–102.

(20) Jia, Q. Q.; Ji, H. M.; Wang, D. H.; Bai, X.; Sun, X. H.; Jin, Z. G. Exposed Facets Induced Enhanced Acetone Selective Sensing Property of Nanostructured Tungsten Oxide. *J. Mater. Chem. A* **2014**, *2*, 13602–13611.

(21) Zhang, N.; Chen, C.; Mei, Z.; Liu, X.; Qu, X.; Li, Y.; Li, S.; Qi, W.; Zhang, Y.; Ye, J.; Roy, V. A. L.; Ma, R. Monoclinic Tungsten Oxide with {100} Facet Orientation and Tuned Electronic Band Structure for Enhanced Photocatalytic Oxidations. *ACS Appl. Mater. Interfaces* **2016**, *8*, 10367–10374.

(22) Dong, P.; Hou, G.; Xi, X.; Shao, R.; Dong, F. WO3-Based Photocatalysts: Morphology Control, Activity Enhancement and Multifunctional Applications. *Environ. Sci. Nano* **2017**, *4*, 539–557.

(23) Zhao, Z. G.; Liu, Z. F.; Miyauchi, M. Nature-Inspired Construction, Characterization, and Photocatalytic Properties of Single-Crystalline Tungsten Oxide Octahedra. *Chem. Commun.* **2010**, *46*, 3321–3323.

(24) Li, Y.; Tang, Z.; Zhang, J.; Zhang, Z. Enhanced Photocatalytic Performance of Tungsten Oxide through Tuning Exposed Facets and Introducing Oxygen Vacancies. *J. Alloys Compd.* **2017**, *708*, 358–366.

(25) Ding, J.; Chai, Y.; Liu, Q.; Liu, X.; Ren, J.; Dai, W. L. Selective Deposition of Silver Nanoparticles onto WO3 Nanorods with Different Facets: The Correlation of Facet-Induced Electron Transport Preference and Photocatalytic Activity. *J. Phys. Chem. C* **2016**, *120*, 4345–4353.

(26) Lin, R.; Wan, J.; Xiong, Y.; Wu, K.; Cheong, W. C.; Zhou, G.; Wang, D.; Peng, Q.; Chen, C.; Li, Y. Quantitative Study of Charge Carrier Dynamics in Well-Defined WO3 Nanowires and Nanosheets: Insight into the Crystal Facet Effect in Photocatalysis. *J. Am. Chem. Soc.* **2018**, *140*, 9078–9082.

(27) Tao, S.; Schmidt, I.; Brocks, G.; Jiang, J.; Tranca, I.; Meerholz, K.; Olthof, S. Absolute Energy Level Positions in Tin- and Lead-Based Halide Perovskites. *Nat. Commun.* **2019**, *10*, 1–10.

(28) Waller, M. R.; Townsend, T. K.; Zhao, J.; Sabio, E. M.; Chamousis, R. L.; Browning, N. D.; Osterloh, F. E. Oxidation in the Quantum Confinement Regime. *Chem. Mater.* **2012**, *24*, 698−704.

(29) Watanabe, H.; Fujikata, K.; Oaki, Y.; Imai, H. Band-Gap Expansion of Tungsten Oxide Quantum Dots Synthesized in Sub-Nano Porous Silica. *Chem. Commun.* **2013**, *49*, 8477–8479.

(30) Tanaka, D.; Oaki, Y.; Imai, H. Enhanced Photocatalytic Activity of Quantum-Confined Tungsten Trioxide Nanoparticles in Mesoporous Silica. *Chem. Commun.* **2010**, *46*, 5286–5288.

(31) Cong, S.; Tian, Y.; Li, Q.; Zhao, Z.; Geng, F. Single-Crystalline Tungsten Oxide Quantum Dots for Fast Pseudocapacitor and Electrochromic Applications. *Adv. Mater.* **2014**, *26*, 4260–4267.

(32) Meda, L.; Tozzola, G.; Tacca, A.; Marra, G.; Caramori, S.; Cristino, V.; Bignozzi, C.A. Photo-Electrochemical Properties of Nanostructured WO3 Prepared with Different Organic Dispersing Agents. *Sol. Energy Mater. Sol. Cells* **2010**, *94*, 788–796.

(33) Shyamal, S.; Dutta, S. K.; Das, T.; Sen, S.; Chakraborty, S.; Pradhan, N. Facets and Defects in Perovskite Nanocrystals for Photocatalytic CO2 Reduction. *J. Phys. Chem. Lett.* **2020**, *11*, 3608–3614.

(34) Liu, X. D.; Wang, Q.; Cheng, Z. Q.; Qiu, Y. H.; Zhou, L.; Wang, Q. Q. Solution-Phase Growth of Organolead Halide Perovskite Nanowires and Nanoplates Assisted by Long-Chain Alkylammonium and Solvent Polarity. *Mater. Lett.* **2017**, *206*, 75–79.

(35) Diez-Cabanes, V.; Morales-Garcia, A.; Illas, F.; Pastore, M. Understanding the Structural and Electronic Properties of Photoactive Tungsten Oxide Nanoparticles from Density Functional Theory and GW Approaches. *J. Chem. Theory Comput.* **2021**, *17*, 3462–3470.

(36) Katan, C.; Mercier, N.; Even, J. Quantum and Dielectric Confinement Effects in Lower-Dimensional Hybrid Perovskite Semiconductors. *Chem. Rev.* **2019**, *119*, 3140–3192.

(37) Li, Y. F.; Feng, J.; Sun, H. B. Perovskite Quantum Dots for Light-Emitting Devices. *Nanoscale* **2019**, *11*, 19119–19139.

(38) Protesescu, L.; Yakunin, S.; Bodnarchuk, M. I.; Krieg, F.; Caputo, R.; Hendon, C. H.; Yang,

R. X.; Walsh, A.; Kovalenko, M. V. Nanocrystals of Cesium Lead Halide Perovskites (CsPbX3, X = Cl, Br, and I): Novel Optoelectronic Materials Showing Bright Emission with Wide Color Gamut. *Nano Lett.* **2015**, *15*, 3692–3696.

(39) Gao, G.; Xi, Q.; Zhou, H.; Zhao, Y.; Wu, C.; Wang, L.; Guo, P.; Xu, J. Novel Inorganic Perovskite Quantum Dots for Photocatalysis. *Nanoscale* **2017**, *9*, 12032–12038.

(40) Lin, J.; Gomez, L.; De Weerd, C.; Fujiwara, Y.; Gregorkiewicz, T.; Suenaga, K. Direct Observation of Band Structure Modifications in Nanocrystals of CsPbBr3 Perovskite. *Nano Lett.* **2016**, *16*, 7198–7202.

(41) Shamsi, J.; Urban, A. S.; Imran, M.; De Trizio, L.; Manna, L. Metal Halide Perovskite Nanocrystals: Synthesis, Post-Synthesis Modifications, and Their Optical Properties. *Chem. Rev.* **2019**, *119*, 3296–3348.

(42) Hou, J.; Cao, S.; Wu, Y.; Gao, Z.; Liang, F.; Sun, Y.; Lin, Z.; Sun, L. Inorganic Colloidal Perovskite Quantum Dots for Robust Solar CO2 Reduction. *Chem. - A Eur. J.* **2017**, *23*, 9481–9485.

(43) Anaya, M.; Rubino, A.; Rojas, T. C.; Galisteo-López, J. F.; Calvo, M. E.; Míguez, H. Strong Quantum Confinement and Fast Photoemission Activation in CH3NH3PbI3 Perovskite Nanocrystals Grown within Periodically Mesostructured Films. *Adv. Opt. Mater.* **2017**, *5*, 1601087.

(44) Butkus, J.; Vashishtha, P.; Chen, K.; Gallaher, J. K.; Prasad, S. K. K.; Metin, D. Z.; Laufersky, G.; Gaston, N.; Halpert, J. E.; Hodgkiss, J. M. The Evolution of Quantum Confinement in CsPbBr3 Perovskite Nanocrystals. *Chem. Mater.* **2017**, *29*, 3644–3652.

(45) Haruyama, J.; Sodeyama, K.; Han, L.; Tateyama, Y. Termination Dependence of Tetragonal CH3NH3PbI 3 Surfaces for Perovskite Solar Cells. *J. Phys. Chem. Lett.* **2014**, *5*, 2903–

2909.

(46) Lee, T.; Lee, Y.; Jang, W.; Soon, A. Understanding the Advantage of Hexagonal WO3 as an Efficient Photoanode for Solar Water Splitting: A First-Principles Perspective. *J. Mater. Chem. A* **2016**, *4*, 11498–11506.

(47) Pham, T. A.; Ping, Y.; Galli, G. Modelling Heterogeneous Interfaces for Solar Water Splitting. *Nat. Mater.* **2017**, *16*, 401–408.

(48) Hörmann, N. G.; Guo, Z.; Ambrosio, F.; Andreussi, O.; Pasquarello, A.; Marzari, N. Absolute Band Alignment at Semiconductor-Water Interfaces Using Explicit and Implicit Descriptions for Liquid Water. *npj Comput. Mater.* **2019**, *100*, 1–6.

(49) Hussain, H.; Tocci, G.; Woolcot, T.; Torrelles, X.; Pang, C. L.; Humphrey, D. S.; Yim, C. M.; Grinter, D. C.; Cabailh, G.; Bikondoa, et al. Structure of a Model TiO2 Photocatalytic Interface. *Nat. Mater.* **2017**, *16*, 461–467.

(50) Andrade, M. F. C.; Ko, H.-Y.; Car, R.; Selloni, A. Structure, Polarization, and Sum Frequency Generation Spectrum of Interfacial Water on Anatase TiO2. *J. Phys. Chem. Lett.* **2018**, *9*, 6716–6721.

(51) Kishore, R.; Cao, X.; Zhang, X.; Bieberle-Hütter, A. Electrochemical Water Oxidation on WO3 Surfaces: A Density Functional Theory Study. *Catal. Today* **2019**, *321–322*, 94–99.

(52) Zhao, L.; Tian, F. H.; Wang, X.; Zhao, W.; Fu, A.; Shen, Y.; Chen, S.; Yu, S. Mechanism of CO Adsorption on Hexagonal WO3 (0 0 1) Surface for Gas Sensing: A DFT Study. *Comput. Mater. Sci.* **2013**, *79*, 691–697.

(53) Albanese, E.; Valentin, C. Di; Pacchioni, G. H2O Adsorption on WO3 and WO3−x (001) Surfaces. *ACS Appl. Mater. Interfaces* **2017**, *9*, 23212–23221.

(54) Mosconi, E.; Azpiroz, J. M.; De Angelis, F. Ab Initio Molecular Dynamics Simulations of

Methylammonium Lead Iodide Perovskite Degradation by Water. *Chem. Mater.* **2015**, *27*, 4885–4892.

(55) Hall, G. N.; Stuckelberger, M.; Nietzold, T.; Hartman, J.; Park, J. S.; Werner, J.; Niesen, B.; Cummings, M. L.; Rose, V.; Ballif, C.; Chan, M. K.; Fenning, D. P.; Bertoni, M. I. The Role of Water in the Reversible Optoelectronic Degradation of Hybrid Perovskites at Low Pressure. *J. Phys. Chem. C* **2017**, *121*, 25659–25665.

(56) Ouyang, Y.; Shi, L.; Li, Q.; Wang, J. Role of Water and Defects in Photo-Oxidative Degradation of Methylammonium Lead Iodide Perovskite. *Small Methods* **2019**, *3*, 2–7.

(57) Wang, L.; Xiao, H.; Cheng, T.; Li, Y.; Goddard, W. A. Pb-Activated Amine-Assisted Photocatalytic Hydrogen Evolution Reaction on Organic-Inorganic Perovskites. *J. Am. Chem. Soc.* **2018**, *140*, 1994–1997.

(58) Lamiel-Garcia, O.; Cuko, A.; Calatayud, M.; Illas, F.; Bromley, S. T. Predicting Size-Dependent Emergence of Crystallinity in Nanomaterials: Titania Nanoclusters: Versus Nanocrystals. *Nanoscale* **2017**, *9*, 1049–1058.

(59) Manzhos, S.; Pal, A.; Chen, Y.; Giorgi, G. Effect of Organic Cation States on Electronic Properties of Mixed Organic-Inorganic Halide Perovskite Clusters. *Phys. Chem. Chem. Phys.* **2019**, *21*, 8161–8169.

(60) Giorgi, G.; Yoshihara, T.; Yamashita, K. Structural and Electronic Features of Small Hybrid Organic-Inorganic Halide Perovskite Clusters: A Theoretical Analysis. *Phys. Chem. Chem. Phys.* **2016**, *18*, 27124–27132.

(61) Vogel, D. J.; Kryjevski, A.; Inerbaev, T.; Kilin, D. S. Photoinduced Single- and Multiple-Electron Dynamics Processes Enhanced by Quantum Confinement in Lead Halide Perovskite Quantum Dots. *J. Phys. Chem. Lett.* **2017**, *8*, 3032–3039.

(62) Neukirch, A. J.; Nie, W.; Blancon, J. C.; Appavoo, K.; Tsai, H.; Sfeir, M. Y.; Katan, C.; Pedesseau, L.; Even, J.; Crochet, et al. Polaron Stabilization by Cooperative Lattice Distortion and Cation Rotations in Hybrid Perovskite Materials. *Nano Lett.* **2016**, *16*, 3809–3816.

(63) Valero, R.; Morales-García, Á.; Illas, F. Theoretical Modeling of Electronic Excitations of Gas-Phase and Solvated TiO2 Nanoclusters and Nanoparticles of Interest in Photocatalysis. *J. Chem. Theory Comput.* **2018**, *14*, 4391–4404.

(64) Naserifar, S.; Chen, Y.; Kwon, S.; Xiao, H. Article Artificial Intelligence and QM/MM with a Polarizable Reactive Force Field for Next- Generation Electrocatalysts. *Matter* **2021**, *4*, 195–216.

(65) Hai, X.; Tahir-Kheli, J.; Goddard, W. A. Accurate Band Gaps for Semiconductors from Density Functional Theory. *J. Phys. Chem. Lett.* **2011**, *2*, 212–217.

(66) Even, J.; Pedesseau, L.; Jancu, J. M.; Katan, C. Importance of Spin-Orbit Coupling in Hybrid Organic/Inorganic Perovskites for Photovoltaic Applications. *J. Phys. Chem. Lett.* **2013**, *4*, 2999–3005.

(67) Adamo, C.; Jacquemin, D. The Calculations of Excited-State Properties with Time-Dependent Density Functional Theory. *Chem. Soc. Rev.* **2013**, *42*, 845–856.

(68) Blase, X.; Duchemin, I.; Jacquemin, D. The Bethe-Salpeter Equation in Chemistry: Relations with TD-DFT, Applications and Challenges. *Chem. Soc. Rev.* **2018**, *47*, 1022–1043.

(69) Giorgi, G.; Yamashita, K.; Palummo, M. Nature of the Electronic and Optical Excitations of Ruddlesden-Popper Hybrid Organic-Inorganic Perovskites: The Role of the Many-Body Interactions. *J. Phys. Chem. Lett.* **2018**, *9*, 5891–5896.

(70) Boyer-Richard, S.; Katan, C.; Traoré, B.; Scholz, R.; Jancu, J. M.; Even, J. Symmetry-Based Tight Binding Modeling of Halide Perovskite Semiconductors. *J. Phys. Chem. Lett.* **2016**, *7*, 3833–3840.

(71) Selli, D.; Fazio, G.; Di Valentin, C. Using Density Functional Theory to Model Realistic TiO2 Nanoparticles, Their Photoactivation and Interaction with Water. *Catalysts* **2017**, *7*, 357.

(72) Liu, H.; Di Valentin, C. Shaping Magnetite Nanoparticles from First Principles. *Phys. Rev. Lett.* **2019**, *123*, 186101.

(73) Pal, S.; Trivedi, D. J.; Akimov, A. V.; Aradi, B.; Frauenheim, T.; Prezhdo, O. V. Nonadiabatic Molecular Dynamics for Thousand Atom Systems: A Tight-Binding Approach toward PYXAID. *J. Chem. Theory Comput.* **2016**, *12*, 1436–1448.

(74) Lin, H.; Truhlar, D. G. QM/MM: What Have We Learned, Where Are We, and Where Do We Go from Here? *Theor. Chem. Acc.* **2007**, *117*, 185–199.

(75) Fazio, G.; Selli, D.; Ferraro, L.; Seifert, G.; Di Valentin, C. Curved TiO2 Nanoparticles in Water: Short (Chemical) and Long (Physical) Range Interfacial Effects. *ACS Appl. Mater. Interfaces* **2018**, *10*, 29943–29953.

(76) He, J.; Vasenko, A. S.; Long, R.; Prezhdo, O. V. Halide Composition Controls Electron-Hole Recombination in Cesium-Lead Halide Perovskite Quantum Dots: A Time Domain Ab Initio Study. *J. Phys. Chem. Lett.* **2018**, *9*, 1872–1879.

(77) Mattoni, A.; Filippetti, A.; Saba, M. I.; Delugas, P. Methylammonium Rotational Dynamics in Lead Halide Perovskite by Classical Molecular Dynamics: The Role of Temperature. *J. Phys. Chem. C* **2015**, *119*, 17421–17428.

(78) Kim, S.-Y.; Kumar, N.; Persson, P.; Sofo, J.; van Duin, A. C. T.; Kubicki, J. D.

Development of a ReaxFF Reactive Force Field for Titanium Dioxide/Water Systems. *Langmuir* **2013**, *29*, 7838–7846.

(79) Jinnouchi, R.; Asahi, R. Predicting Catalytic Activity of Nanoparticles by a DFT-Aided Machine-Learning Algorithm. *J. Phys. Chem. Lett.* **2017**, *8*, 4279–4283.

(80) Zhou, Y.; Zhang, Z.; Fang, Z.; Qiu, M.; Ling, L.; Long, J.; Chen, L.; Tong, Y.; Su, W.; Zhang, Y.; et al. Defect Engineering of Metal-Oxide Interface for Proximity of Photooxidation and Photoreduction. *Proc. Natl. Acad. Sci. U. S. A.* **2019**, *116*, 10232–10237.

(81) Zhang, L. J.; Li, S.; Liu, B. K.; Wang, D. J.; Xie, T. F. Highly Efficient CdS/WO3 Photocatalysts: Z-Scheme Photocatalytic Mechanism for Their Enhanced Photocatalytic H2 Evolution under Visible Light. *ACS Catal.* **2014**, *4*, 3724–3729.

(82) Li, R.; Li, X.; Wu, J.; Lv, X.; Zheng, Y. Z.; Zhao, Z.; Ding, X.; Tao, X.; Chen, J. F. Few-Layer Black Phosphorus-on-MAPbI3 for Superb Visible-Light Photocatalytic Hydrogen Evolution from HI Splitting. *Appl. Catal. B Environ.* **2019**, *259*, 118075.

(83) Mandal, S.; Mukherjee, S.; De, C. K.; Roy, D.; Ghosh, S.; Mandal, P. K. Extent of Shallow/Deep Trap States beyond the Conduction Band Minimum in Defect-Tolerant CsPbBr3 Perovskite Quantum Dot: Control over the Degree of Charge Carrier Recombination. *J. Phys. Chem. Lett.* **2020**, *11*, 1702–1707.

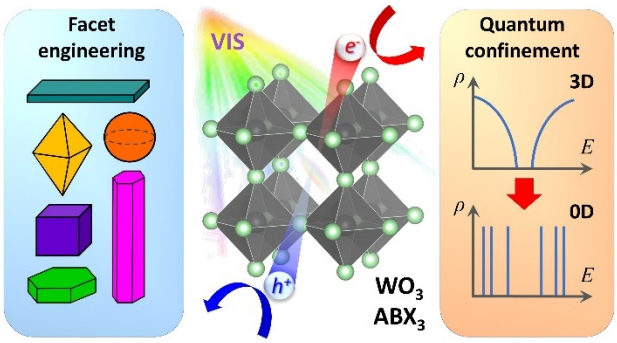

TOC Graphic

Biography

Dr. Valentin Diez-Cabanes obtained his title in Materials Engineering in 2014 from the Technical University of Madrid, having carried out of his Master Thesis at the Department of Electrochemical Materials of the J. Heyrovsky Institute of Physical Chemistry in Prague. From 2015 to 2019, he completed his PhD thesis and his first postdoc at the Laboratory for Chemistry of Novel Materials in the University of Mons, where he was hired as Early Stage Researcher (ESR) in a Marie Skłodowska-Curie Action Innovative Training Network. Nowadays, he is a post-doctoral researcher in the Laboratoire de Physique et Chimie Théoriques (LPCT) group, at the University of Lorraine in Nancy, France. His research is focused on the electronic and optical processes in hybrid inorganic/organic semiconductors and their applications in the fields of opto-electronics and photocatalysis.

Dr. Mariachiara Pastore is a senior CNRS researcher in the Laboratoire de Physique et Chimie Théoriques (LPCT) in Nancy, France. She was the recipient of the “Carla Roetti” prize 2014 from the Italian Chemistry Society (SCI), dedicated to theoretical and computational chemists under 40, and of the Ricercat@mente award in 2013 from the Italian National Research Council (CNR) for the Best Young Researcher under 35 years old in Chemical Science and MaterialsTechnology. She

is an expert in the development and application of ab initio methods to the modelling of the structural, electronic, and optical properties of organic/inorganic hybrid materials and interfaces in the broad field of solar energy and solar fuels devices.